Science Advances
AAAS

advances.sciencemag.org/cgi/content/full/6/7/eaaz1466/DC1

# Supplementary Materials for

## Marked structural rearrangement of mannose 6-phosphate/IGF2 receptor at different pH environments

Rong Wang, Xiaofeng Qi, Philip Schmiege, Elias Coutavas, Xiaochun Li*

*Corresponding author. Email: xiaochun.li@utsouthwestern.edu

Published 12 February 2020, *Sci. Adv.* **6**, eaaz1466 (2020)
DOI: 10.1126/sciadv.aaz1466

**This PDF file includes:**

Fig. S1. Sequence alignment of different domains in IGF2R.
Fig. S2. Biochemical characterization of apo state IGF2R and IGF2-bound IGF2R.
Fig. S3. Data processing and model quality assessment of apo state IGF2R.
Fig. S4. Cryo-EM map of apo state IGF2R.
Fig. S5. Structural comparison for seven subgroups of apo state IGF2R in two different views.
Fig. S6. Data processing for ligand-free IGF2R.
Fig. S7. Data processing and model quality assessment of IGF2-bound IGF2R.
Fig. S8. Cryo-EM map of IGF2-bound IGF2R.
Fig. S9. Structural comparison of CD-MPR and domains of IGF2R for Man6P.
Table S1. Cryo-EM data collection, refinement, and validation statistics.

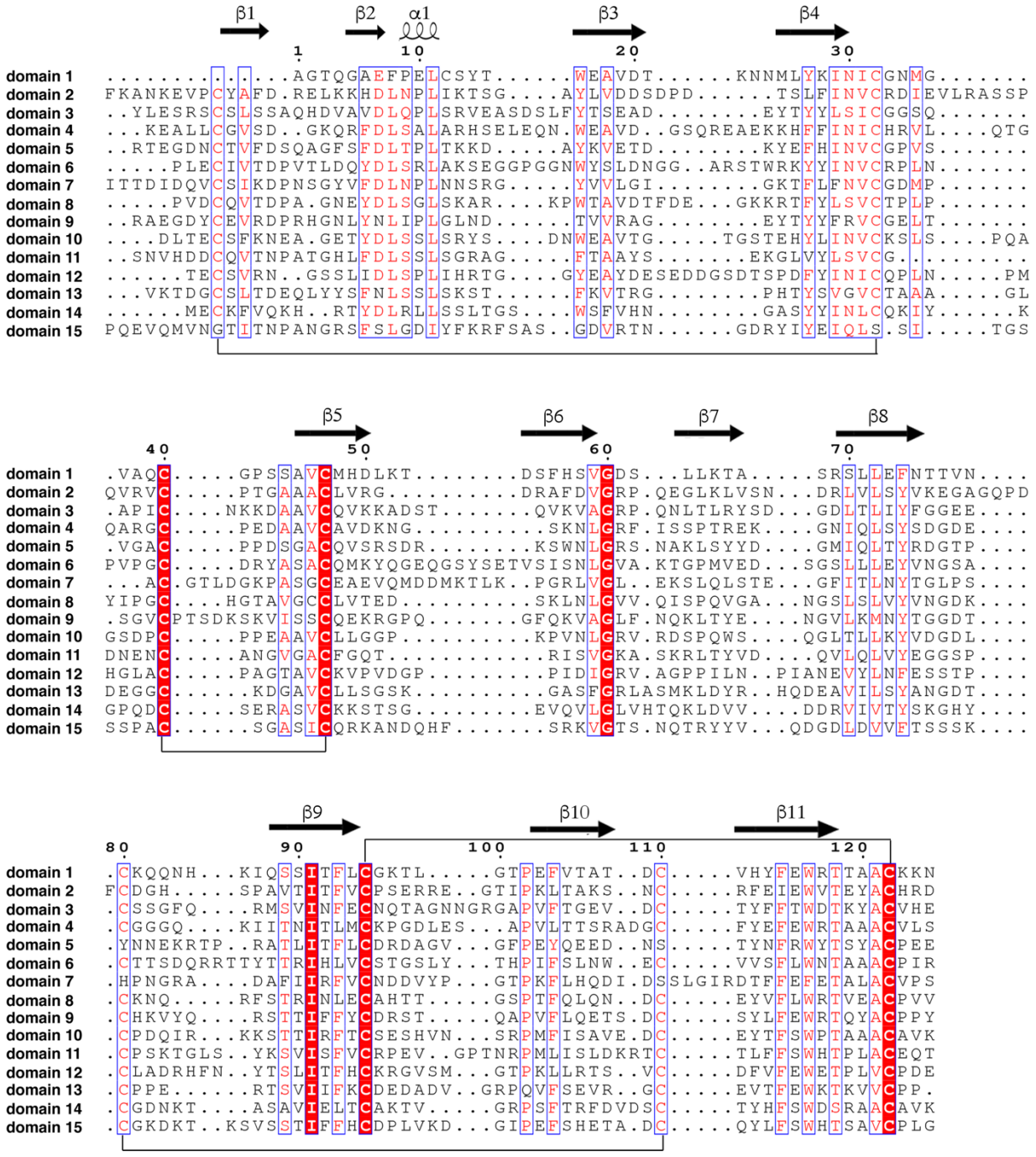


**Fig. S1. Sequence alignment of different domains in IGF2R.** The sequence of domain 13 is listed without FNII domain. Strictly conserved residues are highlighted in shaded red boxes and conserved residues in open red boxes. The secondary structures of a domain are placed on the top of the alignments. The pairs of disulfide bonds are indicated by lines.

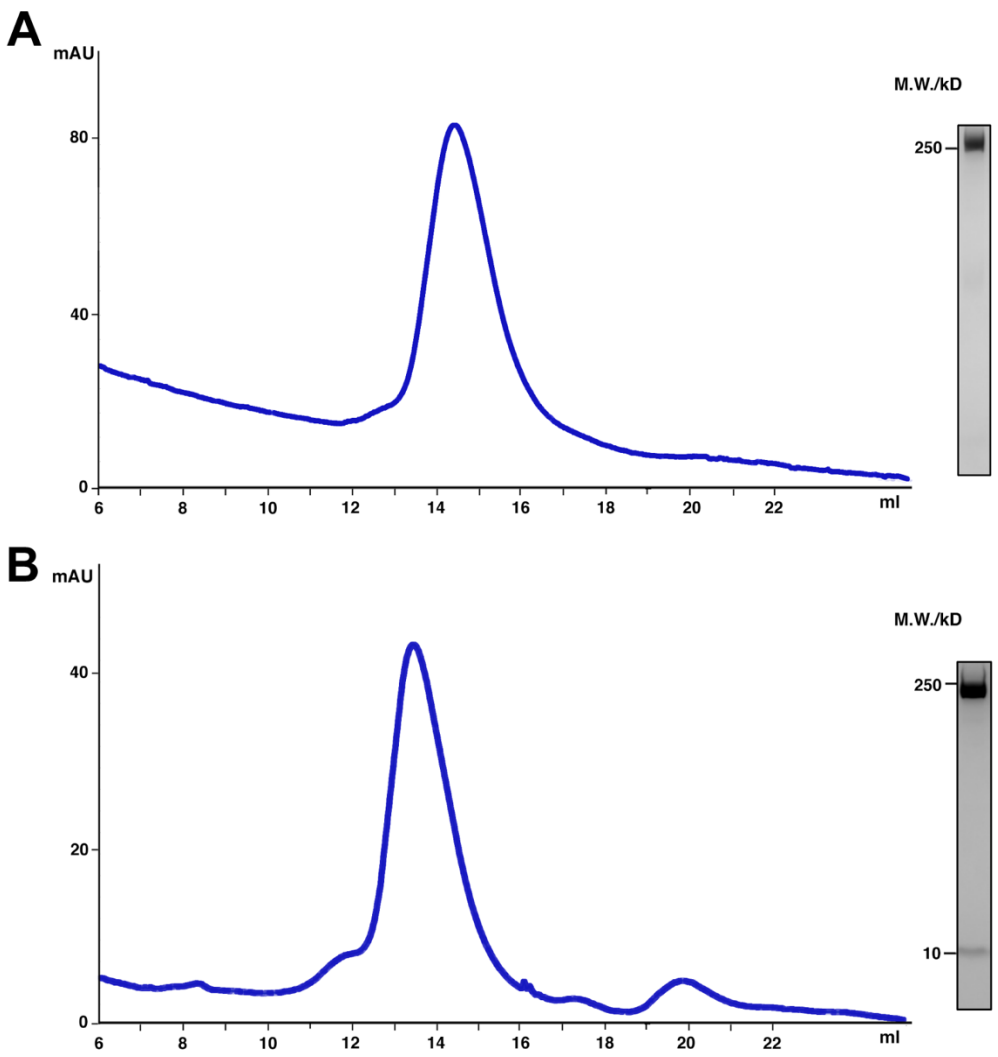


**Fig. S2. Biochemical characterization of apo state IGF2R and IGF2-bound IGF2R.** (**A**) Size-exclusion chromatography of apo state IGF2R at pH 4.5. (**B**) Size-exclusion chromatography of IGF2-bound IGF2R at pH 7.4. The elution peak is analyzed by SDS-PAGE and Coomassie staining. Molecular standards are indicated on the left side of the SDS-PAGE.

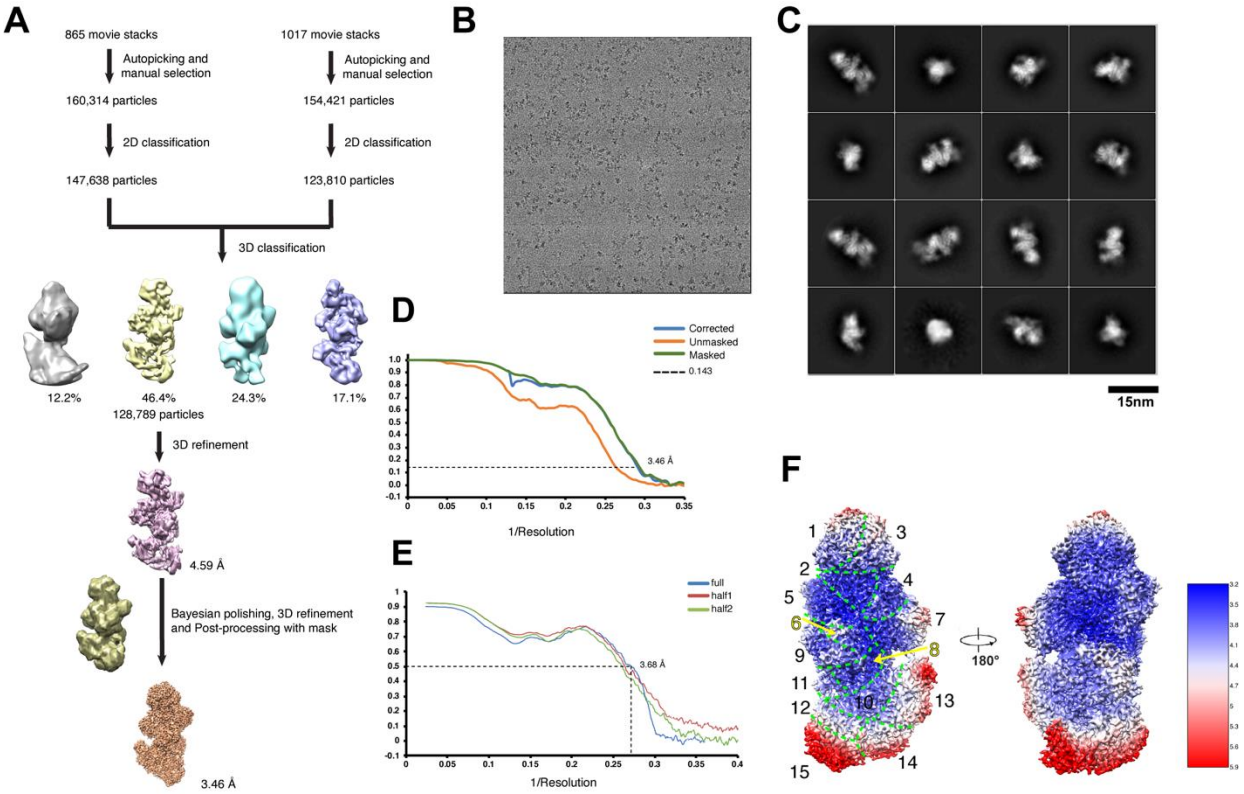


**Fig. S3. Data processing and model quality assessment of apo state IGF2R.** (**A**) The data processing work-flow for apo state IGF2R. (**B**) A representative electron micrograph at -2.0 µm defocus. (**C**) 2D classification for apo state IGF2R. (**D**) Fourier shell correlation (FSC) curve of the structure with FSC as a function of resolution using RELION-3 output. (**E**) FSC curves for cross-validation between the models and the maps. Curves for the final refined model versus the reconstruction from all particles in blue (sum), for the model refined against the reconstruction from only half of the particles versus the same reconstruction in red (work), and for the same model versus the reconstruction from the other half of the particles in green (free). (**F**) Density maps of apo state IGF2R colored by local resolution estimation using RELION-3. Each domain is separated by green dashed lines.

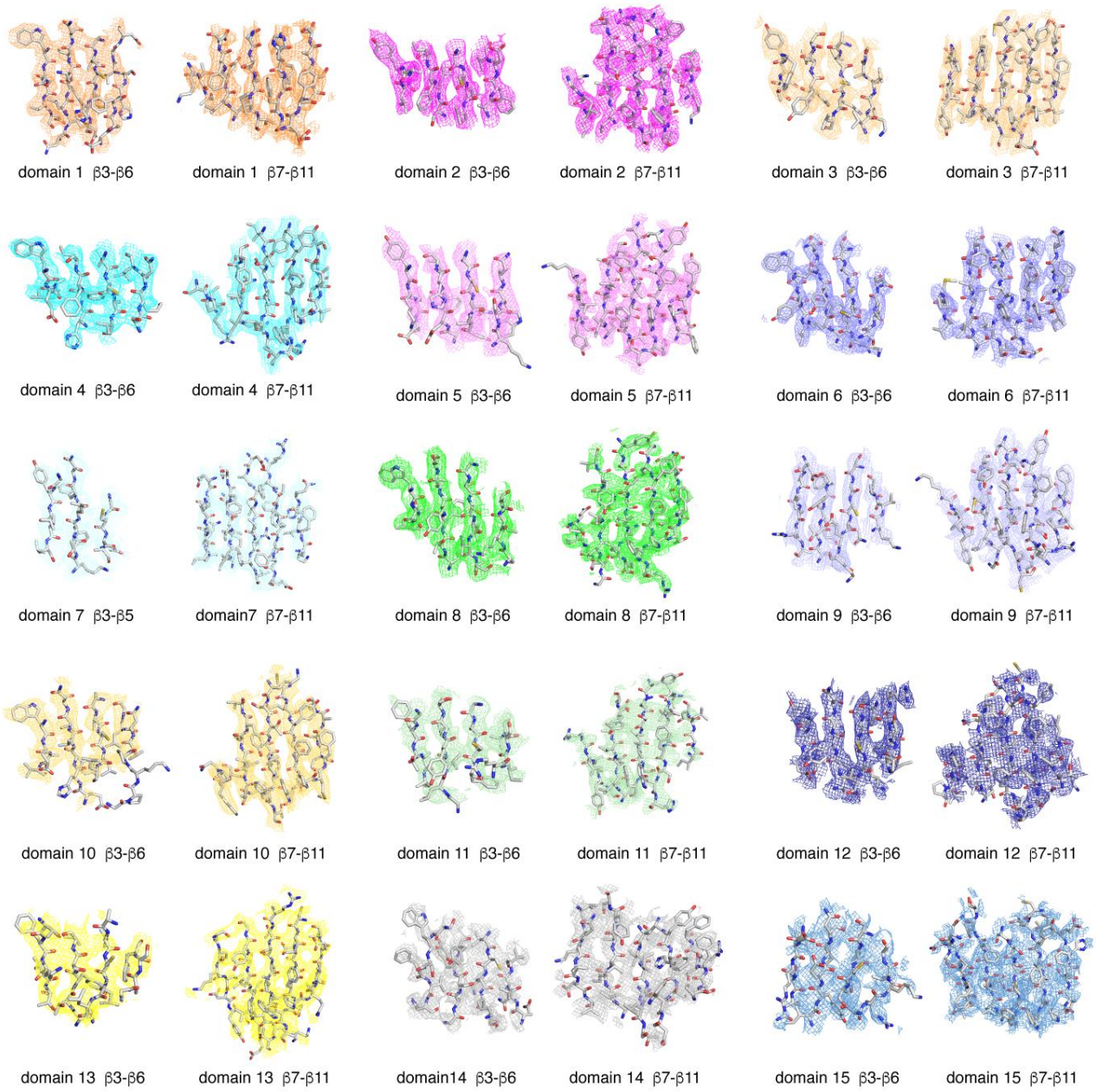


**Fig. S4. Cryo-EM map of apo state IGF2R.** β3-β6 and β7-β11 of each domain are shown. The color scheme of the map is the same as in Fig. 1A.

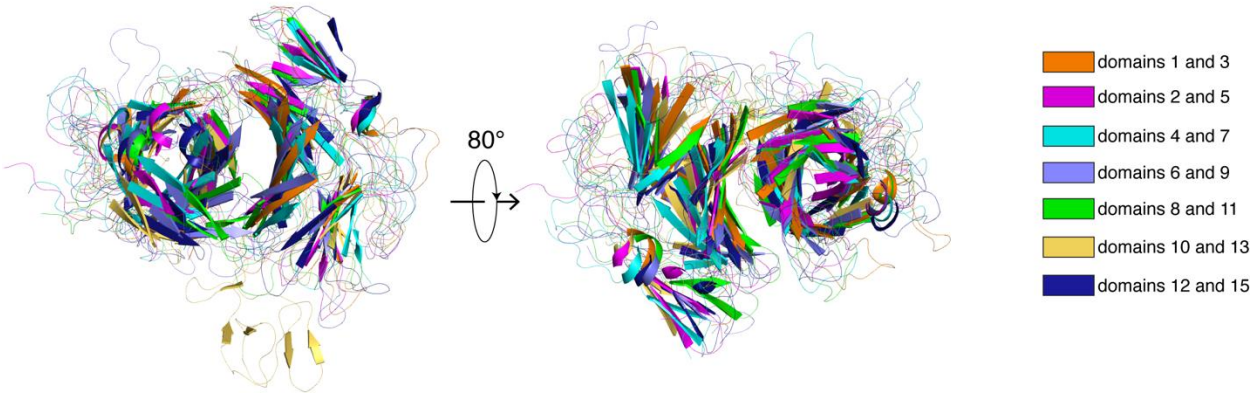


**Fig. S5. Structural comparison for seven subgroups of apo state IGF2R in two different views.** The seven subgroups are shown in different colors as noted in the table on the right side.

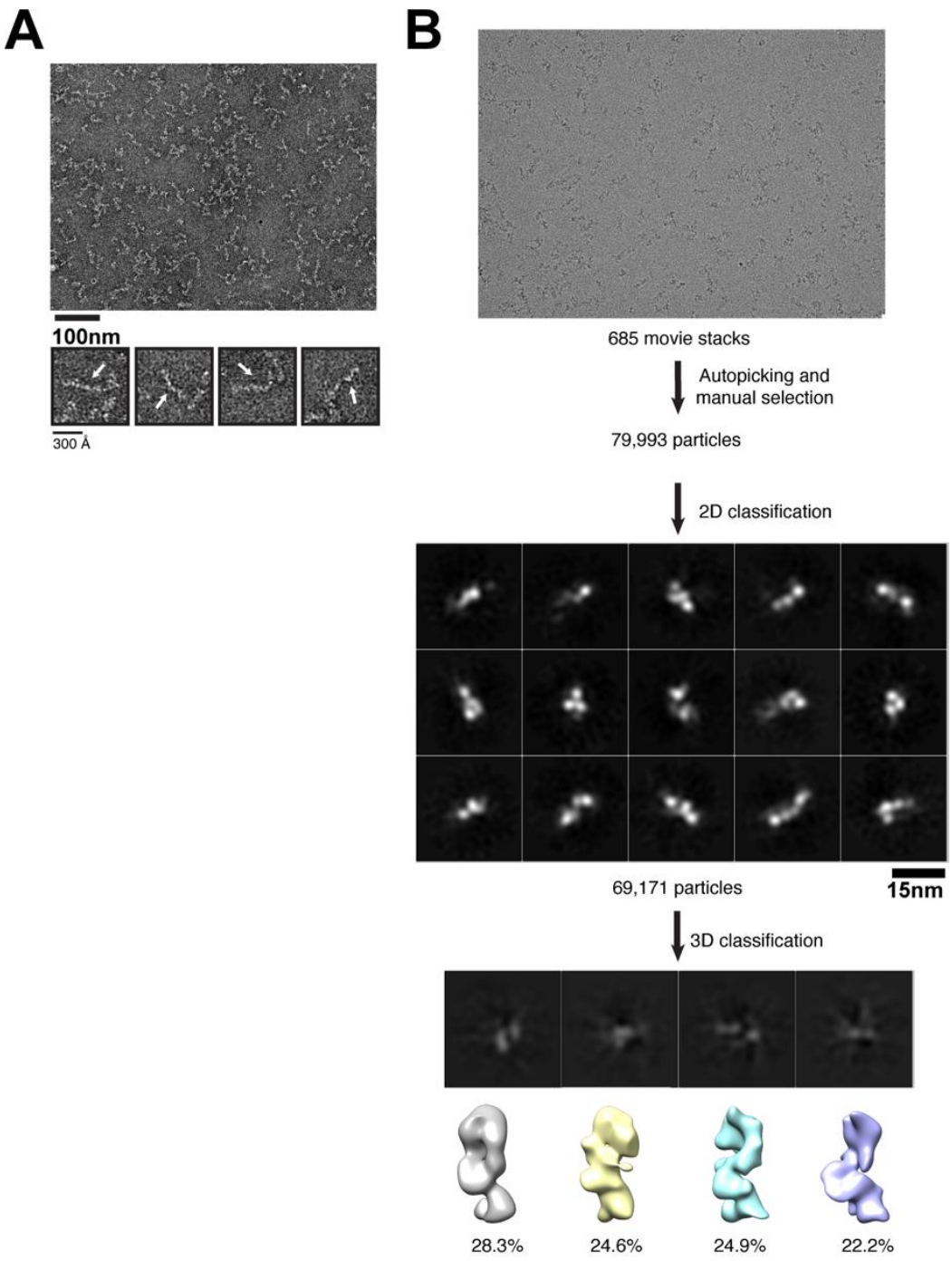


**Fig. S6. Data processing for ligand-free IGF2R.** (**A**) Negative staining image for ligand-free IGF2R at -2.0 µm defocus. The zoomed in images show the extended morphology of IGF2R. The domains are marked with white arrows. (**B**) The data processing work-flow for ligand-free IGF2R with a representative electron micrograph at -2.0 µm defocus.

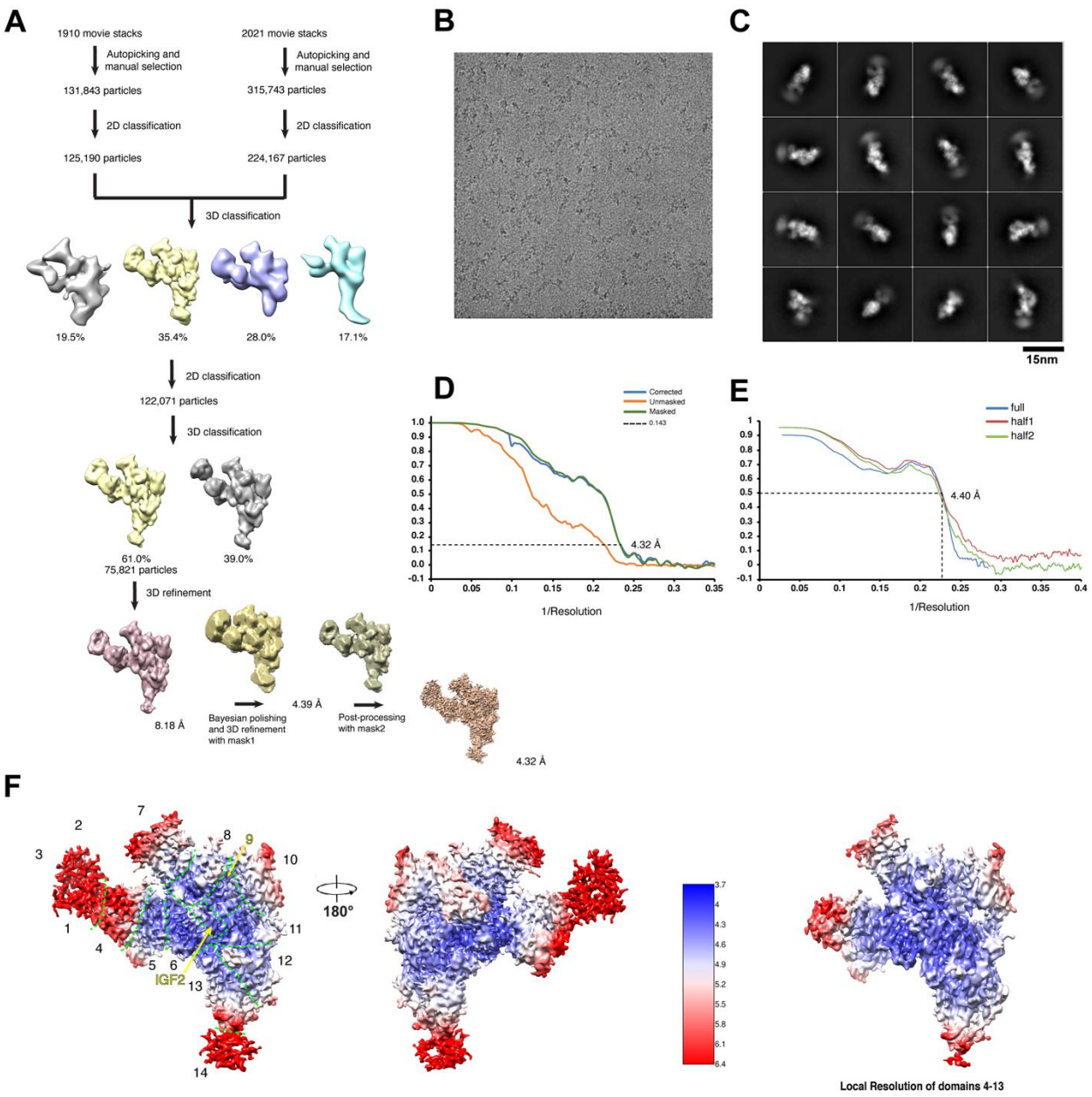


**Fig. S7. Data processing and model quality assessment of IGF2-bound IGF2R.** (**A**) The data processing work-flow for IGF2-bound IGF2R. (**B**) A representative electron micrograph at -2.0 µm defocus. (**C**) 2D classification for IGF2-bound IGF2R. (**D**) Fourier shell correlation (FSC) curve of the structure with FSC as a function of resolution using RELION-3 output. (**E**) FSC curves for cross-validation between the models and the maps. Curves for the final refined model versus the reconstruction from all particles in blue (sum), for the model refined against the

reconstruction from only half of the particles versus the same reconstruction in red (work), and for the same model versus the reconstruction from the other half of the particles in green (free). (**F**) Density maps of IGF2-bound IGF2R colored by local resolution estimation using RELION-3. Each domain is separated by green dashed lines.

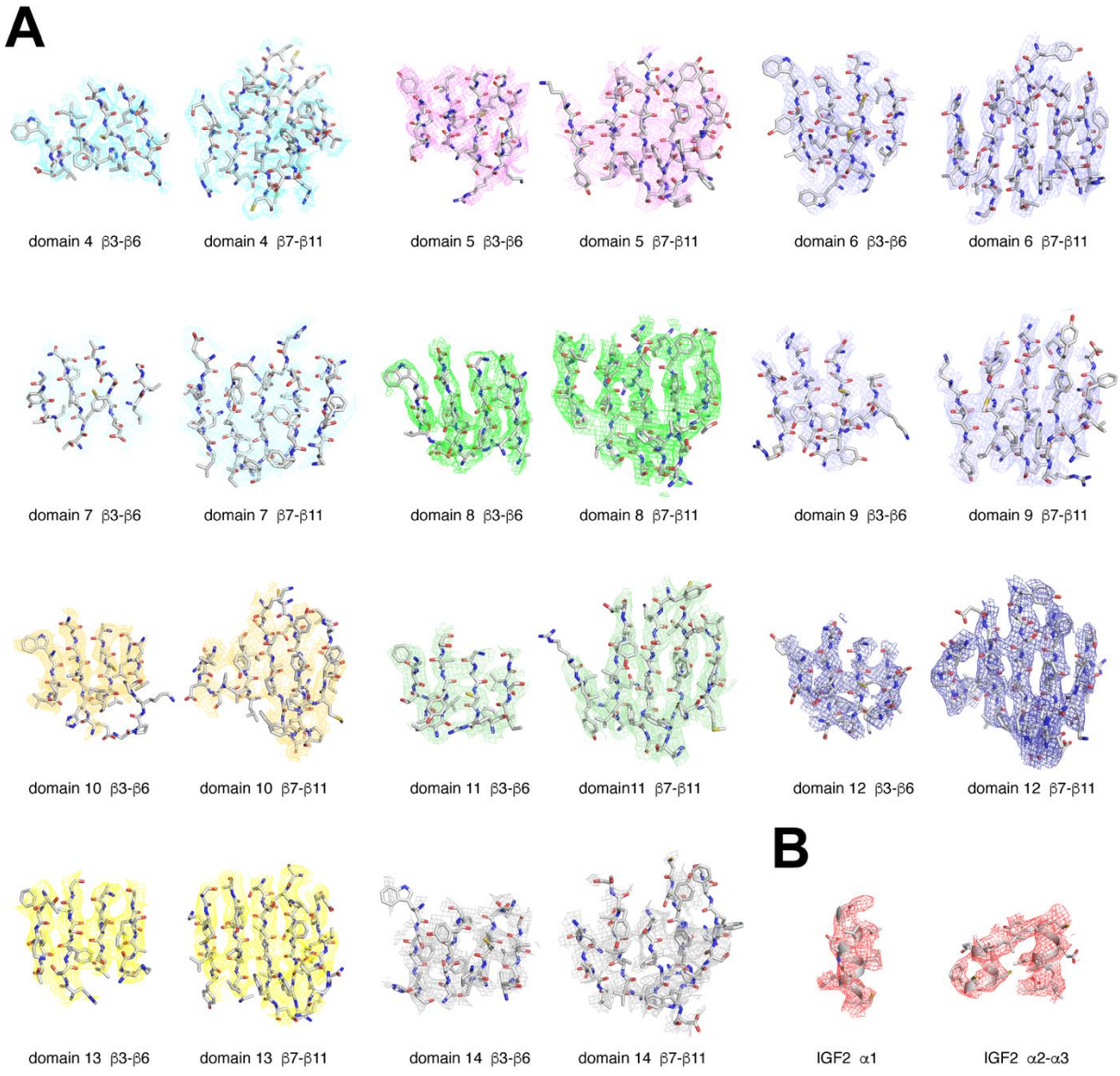


**Fig. S8. Cryo-EM map of IGF2-bound IGF2R.** (**A**) β3-β6 and β7-β11 of the domains 4-14 of IGF2-bound IGF2R. The color scheme of the map is the same as in Fig. 1A. (**B**) α1-α3 of IGF2

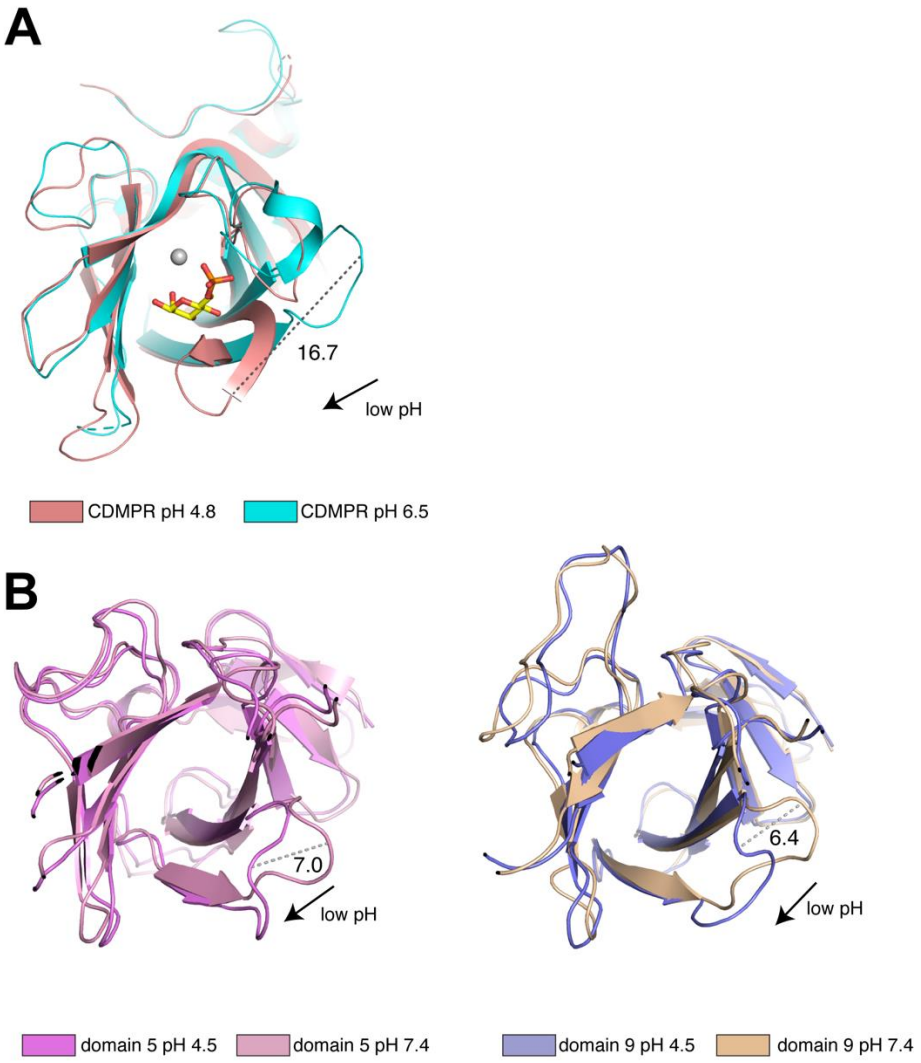


**Fig. S9. Structural comparison of CD-MPR and domains of IGF2R for Man6P.** (**A**) Structural comparison of the lumenal domain of the CD-MPR in different pH. The proteins in pH 4.8 (PDB: 2RL7) and pH 6.5 (PDB: 2RL8) are colored in salmon and cyan, respectively. The bound Man6P and $Mn^{2+}$ are shown with a stick model and a gray sphere, respectively. (**B**) Domain 5 and domain 9 of IGF2R in different pH. Domain 5 and domain 9 at pH 4.5 are colored the same as in Fig. 1A, while domain 5 and domain 9 at pH 7.4 are shown in pink and wheat. The conformational changes of the β10-β11 loops in different pH are indicated with dashed lines.

**Table S1. Cryo-EM data collection, refinement, and validation statistics.**

| | IGF2R (pH 4.5)<br>(EMD-20815)<br>(PDB 6UM1) | IGF2R-IGF2 complex (pH7.4)<br>(EMD-20816)<br>(PDB 6UM2) |
|---|---|---|
| **Data collection and processing** | | |
| Magnification | 50,000 | 58,140 |
| Voltage (kV) | 300 | 300 |
| Electron exposure (e–/Å$^2$) | 80 | 100 |
| Defocus range (μm) | -1.0 to -2.0 | -1.0 to -2.4 |
| Pixel size (Å) | 1 | 0.86 |
| Symmetry imposed | C1 | C1 |
| Initial particle images (no.) | 314,735 | 447,586 |
| Final particle images (no.) | 128,789 | 75,821 |
| Map resolution (Å) | 3.46 | 4.32 |
| FSC threshold 0.143 | | |
| Map resolution range (Å) | 3.2-5.9 | 3.7-6.4 |
| **Refinement** | | |
| Initial model used (PDB code) | Domains 11-14 (2V5O)<br>Domains 1-3 (1Q25)<br>Domain 5 (2VKA) | IGF2R (pH 4.5)<br>Domains 11-14 (2V5O)<br>Domains 11-13-IGF2 (2V5P) |
| Model resolution (Å) | 3.68 | 4.40 |
| FSC threshold 0.5 | | |
| Model resolution range (Å) | 3.68-280.0 | 4.40-302.7 |
| Map sharpening *B* factor (Å$^2$) | -105.2 | -131.20 |
| Model composition | | |
| Non-hydrogen atoms. | 17134 | 13094 |
| Protein residues | 2208 | 1686 |
| Ligands | BMA: 1 NAG: 7 | NAG: 7 |
| *B* factors (Å$^2$) | | |
| Protein | 23.26 | 20.80 |
| Ligand | 17.01 | 26.65 |
| R.m.s. deviations | | |
| Bond lengths (Å) | 0.014 | 0.013 |
| Bond angles (°) | 1.841 | 1.783 |
| Validation | | |
| MolProbity score | 1.95 | 1.97 |
| Clashscore | 9.44 | 9.90 |
| Poor rotamers (%) | 0.95 | 0.62 |
| Ramachandran plot | | |
| Favored (%) | 92.91 | 92.90 |
| Allowed (%) | 6.86 | 6.74 |
| Disallowed (%) | 0.23 | 0.36 |